

Supporting Information

Coordination mechanism of cyanine dyes on the surface of core@active shell β - $\text{NaGdF}_4:\text{Yb}^{3+},\text{Er}^{3+}$ nanocrystals and its role in enhancing upconversion luminescence

Hossein Beygi Nasrabadi ^a, Eduard Madirov ^b, Radian Popescu ^c, Lenka Štacková ^d, Peter Štacko ^d, Petr Klán ^d, Bryce S. Richards ^{a,e}, Damien Hudry ^a, Andrey Turshatov ^a

^a Institute of Microstructure Technology (IMT), Karlsruhe Institute of Technology, Hermann-von-Helmholtz-Platz 1, Eggenstein-Leopoldshafen, 76344, Germany

^b Kazan Federal University, Institute of Physics, 18 Kremlevskaja str., Kazan, 420008, Russia

^c Laboratory of Electron Microscopy, Karlsruhe Institute of Technology, Engesserstrasse 7,
D-76131 Karlsruhe, Germany

^d Department of Chemistry and RECETOX, Masaryk University, Kamenice 5, 625 00 Brno,
Czech Republic

^e Light Technology Institute (LTI), Karlsruhe Institute of Technology, Engesserstrasse 13,
76131 Karlsruhe, Germany

Content

- 1- Materials
 - 2- Synthesis of rare-earth acetate precursors
 - 3- Synthesis of β -NaGdF₄:Yb_{0.18},Er_{0.02} upconversion nanocrystals (UCNCs)
 - 4- Synthesis of β -NaYGd_{0.3}F₄:Yb_{0.18},Er_{0.02} core UCNCs
 - 5- Synthesis of β -NaGdF₄:Yb,Er@NaGdF₄:X core@shell UCNCs
 - 6- Synthesis of cyanine dyes
 - 7- Dye-sensitizing UCNCs
 - 8- Materials characterization
 - 9- Optimal composition of UCNCs
 - 10- Supplementary table
 - 11- Supplementary figures
- References

1- Materials

Gadolinium oxide (Gd_2O_3 , 99.9%, Chempur), yttrium oxide (Y_2O_3 , 99.99%, Chempur), ytterbium oxide (Yb_2O_3 , 99.9%, Chempur), erbium oxide (Er_2O_3 , 99.9%, Chempur), neodymium oxide (Nd_2O_3 , 99.9%, Chempur), acetic acid ($\text{C}_2\text{H}_4\text{O}_2$, glacial, 100%, Merck), acetic anhydride ($\text{C}_4\text{H}_6\text{O}_3$, 99+%, Acros Organics), oleic acid (OA, $\text{C}_{18}\text{H}_{34}\text{O}_2$, technical grade, 90%, Sigma Aldrich), oleylamine (OAm, $\text{C}_{18}\text{H}_{37}\text{N}$, 80-90%, Acros Organics), octadecene (ODE, $\text{C}_{18}\text{H}_{36}$, technical 90%, Sigma Aldrich), sodium hydroxide (NaOH, anhydrous, 98%, Sigma Aldrich), ammonium fluoride (NH_4F , 99.99%, Sigma Aldrich), anhydrous methanol (CH_4O , Acros Organics), toluene (C_7H_8 , Sigma Aldrich), hydrochloric acid (HCl, 37%, CARL ROTH), diethyl ether ($\text{C}_4\text{H}_{10}\text{O}$, 99.5%, Acros Organics), methanol (MeOH, CH_4O , Merck), deuterated methanol (CD_3OD , Deutero). Reagents and solvents for the synthesis of the cyanine dyes of the highest purity available were used as purchased (Sigma Aldrich), or they were purified/dried using standard methods when necessary. The cyanine dyes were synthesized according to the published procedures¹ or purchased from Sigma-Aldrich (Cy 784, i.e., Cardiogreen (ICG)). All materials were used as received. Note that sodium hydroxide, ammonium fluoride, anhydrous methanol, OA, OAM, and ODE are stored under inert conditions in a glovebox under dry nitrogen ($\text{O}_2 < 1 \text{ ppm}$, $\text{H}_2\text{O} < 1 \text{ ppm}$).

Theoretical calculations of projected molecular areas were performed using the Gaussian 16 (Revision A.03)². DFT optimizations were carried out using the Becke three-parameters exchange function in combination with the Lee-Yang-Parr correlation functional (B3LYP). The basis set used for these optimizations was 6-31G(d,p) in the gas phase. Optimized geometries were confirmed to be stationary points by analysis of their vibrational frequencies.

2- Synthesis of rare-earth acetate precursors

Gadolinium acetate ($\text{Gd}(\text{OOCCH}_3)_3 \cdot x\text{H}_2\text{O}$), yttrium acetate ($\text{Y}(\text{OOCCH}_3)_3 \cdot x\text{H}_2\text{O}$), ytterbium acetate ($\text{Yb}(\text{OOCCH}_3)_3 \cdot x\text{H}_2\text{O}$), erbium acetate ($\text{Er}(\text{OOCCH}_3)_3 \cdot x\text{H}_2\text{O}$), and neodymium acetate

(Nd(OOCCH₃)₃.xH₂O) were prepared by adding 20 mmol of rare-earth oxides (RE₂O₃, R= Y, Yb, and Er, respectively) to 25 mL of glacial acetic acid and 50 mL of distilled water in a 250 mL round bottom flask equipped with a reflux condenser. The stirred suspension was heated up to 93 °C under air until the solid oxide was completely dissolved, and a clear colorless solution was obtained (3-24 hours, 93 °C). After cooling, the solution was filtered, and the solvent evaporated with a rotary evaporator at 60 °C for 90 min. The obtained wet powder was dried under vacuum at 60 °C for 6 hours to prepare hydrated rare-earth acetate powders. To further dry the precursors, such hydrated acetates were subsequently added to 50 mL of glacial acetic acid in a three-neck vessel, equipped with a reflux condenser and a dropping funnel containing 10 mL acetic anhydride. The stirred suspension was heated up to 115 °C under Ar atmosphere; then acetic anhydride was added to the mixture very slowly by the dropping funnel. The mixture was heated up to 122 °C under Ar atmosphere (2 hours) until the water was completely reacted. After cooling, the solvent was evaporated with a rotary evaporator at 60 °C for 90 min. The obtained powders were dried under vacuum at 60 °C for 24 hours. The dry powder was stored under inert conditions in a glovebox under dry nitrogen (O₂ < 1 ppm, H₂O < 1 ppm).

3- Synthesis of NaGdF₄:Yb³⁺,Er³⁺ (β-NaGd_{0.8}F₄:Yb_{0.18},Er_{0.02}) upconversion nanocrystals (UCNCs)

Monodisperse β-NaGd_{0.8}F₄:Yb_{0.18}, Er_{0.02} UCNCs were synthesized by the method reported by Wang *et al.*, with some modifications^{3, 4}. The synthesis was performed using the air-free techniques (Schlenk line and glovebox) under purified nitrogen (glovebox) or argon (Schlenk line).

In a 250 mL round bottom flask, the mixture of 3.280 mmol gadolinium acetate, 0.738 mmol ytterbium acetate, and 0.082 mmol erbium acetate together with oleic acid (40 mL), oleylamine (20 mL), and octadecene (60 mL) is heated up to 140 °C (under Ar) to dissolve lanthanide

acetates. After 25 minutes, the temperature is decreased to 100 °C, and the optically clear solution is purified under vacuum. The purification process consists of repeating the vacuum (to 4×10^{-2} mbar) and Ar filling steps ten times, followed by a dynamic vacuum step (to 5×10^{-4} mbar) for 10 minutes.

The resulting solution cooled down to room temperature, then the mixture of sodium hydroxide (10.3 mmol) in 20 mL MeOH and ammonium fluoride (16.5 mmol) in 40 mL MeOH immediately injected into the solution under Ar (Note that two MeOH solutions were prepared in a dry glovebox under N₂, were vortexed for 15 min for complete dissolution, and mixed just before injection into the solution). The resulting solution is heated up to 50 °C under Ar for 30 minutes, then MeOH is evaporated through 30 times vacuuming (to 4×10^{-2} mbar) and Ar filling steps. The final step for the synthesis of β -NaGdF₄:Yb,Er UCNCs is heating the solution to 300 °C for 90 min. After that, the heating mantle is removed, and the flask is left to cool naturally to room temperature.

As-synthesized UCNCs were split into six 50 mL centrifuge tubes (~20 mL per tube) and centrifuged (6797 xg, 5 min), in such a way that white precipitate separated from the clear yellowish supernatant. The supernatant was discarded, and the resulting white precipitates were dispersed in 2 mL toluene. Solutions obtained from the six centrifuge tubes were combined into one centrifuge tube. Then, 35 mL of acetone was added, so that the clear colorless solution turns white turbid. After centrifuging (2655 xg, 3 min), a clear colorless supernatant and white precipitate were obtained. Again, the supernatant was discarded, the white precipitates were dispersed in 10 mL toluene, 35 mL of acetone was added, and the mixture was centrifuged (2655 xg, 3 min). Finally, the supernatant was discarded and the purified UCNCs were dispersed in 10 mL toluene and stored in a tightly closed glass vial.

4- Synthesis of NaY(Gd)F₄:Yb³⁺,Er³⁺ (β -NaY_{0.5}Gd_{0.3}F₄:Yb_{0.18},Er_{0.02}) core UCNCs

The initial precursor solution consists of a mixture of 0.2050 mmol yttrium acetate, 0.1230 mmol gadolinium acetate, 0.0738 mmol ytterbium acetate, 0.0082 mmol erbium acetate

together with 4 mL oleic acid, and 6 mL octadecene in a 50 mL round bottom flask. The solution was heated up to 140 °C (25 min, under Ar), purified at 100 °C (with a similar method as described in section 3), and cooled down to room temperature. In the next step, the mixture of sodium hydroxide (1.03 mmol) in 2 mL MeOH and ammonium fluoride (1.65 mmol) in 4 mL MeOH immediately injected into the solution under Ar (The MeOH solutions were prepared in a glovebox, with a similar method as described in section 3). The resulting solution is heated up to 50 °C (30 min, under Ar), then MeOH was evaporated through 10 times vacuuming (to 4×10^{-2} mbar) and Ar filling steps. The resulting solution is heated up to 280 °C (90 min, under Ar). After that, the heating mantle is removed, and the flask is left to cool naturally to room temperature. As-synthesized UCNCs were centrifuged (6797 xg, 5 min), in such a way that white precipitate separated from the clear yellowish supernatant. The supernatant was discarded, and the resulting white precipitate was dispersed in 1 mL toluene. Then, 15 mL of acetone was added, so that the clear colorless solution turns white turbid. After centrifuging (2655 xg, 3 min), a clear colorless supernatant and white precipitate were obtained. Again, the supernatant was discarded, the white precipitates were dispersed in 1 mL toluene, 15 mL of acetone was added, and the mixture was centrifuged (2655 xg, 3 min). Finally, the supernatant was discarded, and the purified UCNCs were dispersed in 1 mL toluene and stored in a tightly closed glass vial.

5- Synthesis of NaGdF₄:Yb³⁺,Er³⁺@NaGdF₄:Ln³⁺ core@shell UCNCs

In this section, as-synthesized β -NaGd_{0.8}F₄:Yb_{0.18}, Er_{0.02} UCNCs are coated with the active NaGdF₄ shells which are doped with 10% Yb³⁺, 30% Nd³⁺ and 10% Yb³⁺ + 30% Nd³⁺, respectively. In order to prepare comparable core@shell UCNCs, all NaGdF₄:Yb³⁺,Er³⁺ seeds utilized for the subsequent growth shell layers were obtained from one single batch synthesis. The only variable of the synthesis of core@shell UCNCs is the type and concentration of

dopant, while the other growth parameters (e.g., controlled hot-injection, temperature, time, and injection rate) are exactly the same.

Synthesis of NaGdF₄:Yb³⁺,Er³⁺@NaGdF₄:10%Yb³⁺ core@shell UCNCs: In a 50 mL round bottom flask, a mixture of 0.36 mmol gadolinium acetate and 0.04 mmol ytterbium acetate within 4 mL oleic acid and 6 mL octadecene was heated up to 140 °C (under Ar) to dissolve acetate precursors. After 20 minutes, the temperature was decreased to 100 °C, and the optically clear solution was purified under vacuum. The purification process consisted of repeating the vacuum (to 4×10⁻² mbar) and Ar filling steps five times, followed by a dynamic vacuum step (to 5×10⁻⁴ mbar) for 10 minutes. The resulting solution cooled down to room temperature, then the mixture of sodium hydroxide (1.03 mmol) in 2 mL MeOH and ammonium fluoride (1.65 mmol) in 4 mL MeOH immediately injected into the solution under Ar (The MeOH solutions were prepared in a glovebox, by the same method reported for NaGdF₄:Yb³⁺,Er³⁺ core UCNCs). The resulting solution was heated up to 50 °C under Ar for 30 minutes, then MeOH was evaporated through 10 times vacuuming (to 4×10⁻² mbar) and Ar filling steps. The obtained solution was stored into a 10 mL disposable syringe equipped with a stainless steel needle and kept under static Ar (shell precursor solution). For the preparation of seeds solution, a mixture of 0.4 mL of NaGdF₄:Yb³⁺,Er³⁺ UCNCs within 4 mL oleic acid, and 6 mL octadecene was heated up to 100 °C (under Ar) and then purified under vacuum. The purification process consisted of repeating the vacuum (to 4×10⁻² mbar) and Ar filling steps five times. The seeds solution was heated up to 280 °C (under Ar), then the shell precursor solution was slowly injected (300 μL/min) into the seeds solution. The aging step took 60 min long. After that, the heating mantle is removed, and the flask is left to cool naturally to room temperature. As-synthesized NaGdF₄:Yb³⁺,Er³⁺@NaGdF₄:10%Yb³⁺ UCNCs were purified same to that described in section 4, and stored in 0.4 mL toluene.

Synthesis of β-NaGdF₄:Yb³⁺,Er³⁺@NaGdF₄:30%Nd³⁺ core@shell UCNCs: 0.28 mmol gadolinium acetate and 0.12 mmol neodymium acetate in a mixture of oleic acid (4 mL) and

octadecene (6 mL) are heated up to 140 °C (20 minutes, under Ar), purified under vacuum, and cooled down to room temperature. Then the mixture of sodium hydroxide (1.0 mmol) and ammonium fluoride (1.6 mmol) in MeOH is quickly injected, and the solution is heated up to 50 °C for further MeOH evaporation (The MeOH solutions preparation and MeOH evaporation process were done according to the method described in section 3). The obtained solution is subsequently injected into the hot solution of 0.4 mL of NaGdF₄:Yb³⁺,Er³⁺ UCNCs in oleic acid (4 mL), and octadecene (6 mL). The injection process was performed at a slow rate of 300 μL/min at 280 °C (under Ar). After 60 minutes of aging, the heating mantle is removed, and the flask is left to cool naturally to room temperature. As-synthesized UCNCs were purified the same as that described in section 4 and stored in 0.4 mL toluene.

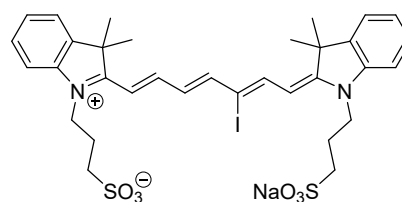
Synthesis of β-NaGdF₄:Yb³⁺,Er³⁺@NaGdF₄:30%Nd³⁺,10%Yb³⁺ core@shell UCNCs: 0.24 mmol gadolinium acetate, 0.12 mmol neodymium acetate, and 0.04 mmol ytterbium acetate in a mixture of oleic acid (4 mL) and octadecene (6 mL) are heated up to 140 °C (20 minutes, under Ar), purified under vacuum, and cooled down to room temperature. Then the mixture of sodium hydroxide (1.0 mmol) and ammonium fluoride (1.6 mmol) in MeOH is quickly injected, and the solution is heated up to 50 °C for further MeOH evaporation (The MeOH solutions preparation and MeOH evaporation process were done according to the method described in section 3). The obtained solution is subsequently injected into the hot solution of 0.4 mL of β-NaGdF₄:Yb,Er UCNCs in oleic acid (4 mL), and octadecene (6 mL). The injection process was performed at a slow rate of 300 μL/min at 280 °C (under Ar). After 60 minutes of aging, the heating mantle is removed, and the flask is left to cool naturally to room temperature. As-synthesized UCNCs were purified the same as that described in section 4 and stored in 0.4 mL toluene.

6- Synthesis of cyanine dyes

The heptamethine cyanines were prepared according to the previously reported method.⁵ The spectroscopic data of Cy 748, 754, 778, and 792 matched those reported therein.

Sodium 3-((*E*)-2-((*2Z,4E,6E*)-7-(3,3-Dimethyl-1-(3-sulfonatopropyl)-3*H*-indol-1-ium-2-yl)-3-iodohepta-2,4,6-trien-1-ylidene)-3,3-dimethylindolin-1-yl)propane-1-sulfonate (Cy 740).

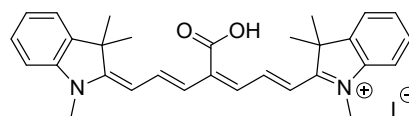
1-(2,4-Dinitrophenyl)-3-iodopyridinium *p*-toluenesulfonate (300 mg, 0.55 mmol) and 4-bromoaniline (143 mg, 0.83 mmol) were dissolved in methanol (5.5 mL), and the mixture



was stirred for 30 min. Subsequently, 3-(2,3,3-trimethyl-3*H*-indolium-1-yl)propane-1-sulfonate (388 mg, 1.38 mmol) and sodium acetate (272 mg, 3.31 mmol) were added, and the reaction mixture was stirred for an additional 16 h at room temperature. Afterwards, diethyl ether (15 mL) was added, and the mixture was placed in a freezer (−16 °C). The resulting precipitate was filtered, washed with diethyl ether (2 × 5 mL) and dried. The crude product was purified by flash column chromatography (silica gel, dichloromethane/methanol with gradient from 20:1 to 5:1). Yield: 233 mg (54%). Dark-green solid. ¹H NMR (500 MHz, *d*₄-CD₃OD): δ (ppm) 8.19 (dd, *J*₁ = 13.6 Hz, *J*₂ = 12.8 Hz, 1H), 7.77 (d, *J* = 12.8 Hz, 1H), 7.68 (d, *J* = 12.5 Hz, 1H), 7.57–7.49 (m, 2H), 7.49–7.40 (m, 2H), 7.39–7.30 (m, 3H), 7.25–7.17 (m, 1H), 6.79 (dd, *J*₁ = 12.3 Hz, *J*₂ = 12.3 Hz, 1H), 6.70 (d, *J* = 14.2 Hz, 1H), 6.26 (d, *J* = 12.8 Hz, 1H), 4.42 (t, *J* = 7.9 Hz, 2H), 4.28 (t, *J* = 7.5 Hz, 2H), 3.08–2.92 (m, 4H), 2.36–2.21 (m, 4H), 1.72 (s, 6H), 1.67 (s, 6H). ¹³C NMR (125 MHz, *d*₄-CD₃OD): δ (ppm) 176.8, 172.9, 158.3, 155.6, 152.2, 143.9, 143.22, 143.16, 142.0, 130.1, 130.0, 129.8, 127.5, 125.8, 123.5, 123.4, 113.2, 111.8, 107.8, 106.2, 96.1, 51.4, 50.3, 49.7, 49.3, 44.6, 44.1, 28.0, 27.8, 24.5, 24.0. HRMS (ESI[−]) *m/z*: [M − Na⁺] calcd for C₃₃H₃₈IN₂O₆S₂[−] 749.1221, found 749.1217.

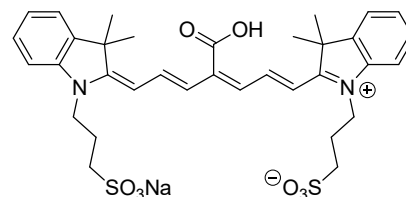
2-((1*E*,3*Z*,5*E*)-4-Carboxy-7-((*E*)-1,3,3-trimethylindolin-2-ylidene)hepta-1,3,5-trien-1-yl)-1,3,3-trimethyl-3*H*-indol-1-ium Iodide (Cy 748).

Green solid. Mp. 142–146 °C (decomp.). ¹H NMR (500 MHz, *d*₄-CD₃OD): δ (ppm) 8.10 (dd, *J*₁ = 13.7 Hz, *J*₂ = 13.7 Hz, 2H), 7.45 (d, *J* = 7.3 Hz, 2H), 7.37 (dd, *J*₁ = 7.6 Hz, *J*₂ = 7.6 Hz, 2H), 7.21 (m, 4H), 6.31 (d, *J* = 13.2 Hz, 2H), 6.22 (d, *J* = 13.6 Hz, 2H), 3.57 (s, 6H), 1.66 (s, 12H). ¹³C NMR (125 MHz, *d*₄-CD₃OD): δ (ppm) 174.6, 173.7, 168.6, 150.5, 144.5, 142.4, 129.6, 125.8, 123.3, 123.0, 111.4, 104.5, 31.3, 28.3.



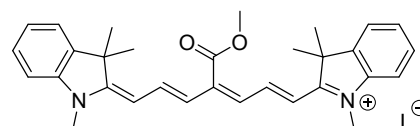
Sodium 3-(2-((1*E*,3*Z*,5*E*)-4-carboxy-7-((*E*)-3,3-dimethyl-1-(3-sulfonatopropyl)indolin-2-ylidene)hepta-1,3,5-trien-1-yl)-3,3-dimethyl-3*H*-indol-1-ium-1-yl)propane-1-sulfonate (Cy 754).

Green solid. Mp. 178–180 °C. ¹H NMR (500 MHz, D₂O): δ (ppm) 8.08 (dd, *J*₁ = 22.1, *J*₂ = 22.1 Hz, 2H), 7.43 (d, *J* = 13.0 Hz, 2H), 7.40–7.31 (m, 4H), 7.25–7.15 (m, 2H), 6.38 (dd, *J*₁ = 23.4, *J*₂ = 23.4 Hz, 4H), 4.26 (t, *J* = 13.2 Hz, 4H), 3.02 (t, *J* = 11.8 Hz, 4H), 2.31–2.18 (m, 4H), 1.63 (s, 12H). ¹³C NMR (125 MHz, D₂O): δ (ppm) 174.8, 172.1, 163.9, 148.1, 142.1, 141.4, 128.6, 124.9, 122.4, 121.5, 110.6, 103.8, 48.9, 48.0, 42.2, 27.3, 22.3.



2-((1*E*,3*Z*,5*E*)-4-(Methoxycarbonyl)-7-((*E*)-1,3,3-trimethylindolin-2-ylidene)hepta-1,3,5-trien-1-yl)-1,3,3-trimethyl-3*H*-indol-1-ium Iodide (Cy 778).

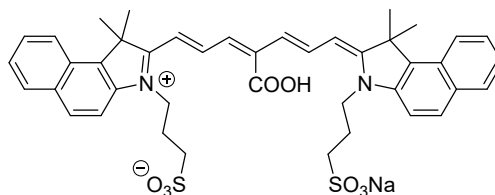
Green solid. Mp. 161–164 °C. ¹H NMR (500 MHz, CDCl₃): δ (ppm) 8.16 (d, *J* = 13.1 Hz, 2H), 7.40–7.33 (m, 4H), 7.23 (t, *J* = 7.3 Hz, 2H), 7.14 (d, *J* = 7.9 Hz, 2H), 7.01 (d, *J* = 12.9 Hz, 2H), 6.72 (d, *J* = 13.5 Hz, 2H), 3.97 (s, 3H), 3.78 (s, 6H), 1.68 (s, 12H). ¹³C NMR (125 MHz, CDCl₃): δ (ppm) 172.6, 167.5, 147.3, 146.0, 143.1, 141.3, 128.9, 125.5, 124.6, 122.4, 110.9, 107.6, 52.7, 49.4, 33.2, 28.2.



Sodium 3-(2-((1*E*,3*Z*,5*E*,7*E*)-4-carboxy-7-(1,1-dimethyl-3-(3-sulfonatopropyl)-1,3-dihydro-2*H*-benzo[*e*]indol-2-ylidene)hepta-1,3,5-trien-1-yl)-1,1-dimethyl-1*H*-benzo[*e*]indol-3-ium-3-yl)propane-1-sulfonate

(Cy 792).

Green solid. Mp. 231–235 °C. ¹H NMR (500 MHz, *d*₄-CD₃OD): δ (ppm) 8.29–8.18 (m, 4H), 7.97 (d, *J* =



8.9 Hz, 2H), 7.95 (d, *J* = 8.0 Hz, 2H), 7.67 (d, *J* = 8.9 Hz, 2H), 7.63–7.58 (m, 2H), 7.46–7.42 (m, 2H), 6.47–6.40 (m, 4H), 4.39 (t, *J* = 7.7 Hz, 4H), 3.03 (t, *J* = 6.9 Hz, 4H), 2.34–2.24 (m, 4H), 1.97 (s, 12H). ¹³C NMR (125 MHz, *d*₄-CD₃OD): δ (ppm) 174.8, 174.4, 167.8, 149.7, 141.1, 134.8, 133.3, 131.7, 131.1, 129.5, 128.6, 125.8, 123.5, 123.3, 112.1, 104.4, 52.1, 49.3, 43.9, 28.0, 24.4.

7- Dye-sensitizing UCNCs

A common protocol was applied to ensure repeatability and reproducibility of results:

- Firstly, one batch of OA-formed UCNCs was used to compare OA-formed UCNCs and Cy-sensitised UCNCs. Briefly, the OA-sensitised UCNCs were divided into several parts. One part (OA-formed UCNCs) was stored in a glove box and used for optical characterization and growing core/shell UCNCs. The second part was washed using HCl solution (OA was removed) and the resulting precipitate (hydrophilic UCNCs) was also stored in a glove box. The same weight of hydrophilic UCNCs was later redispersed and conjugated with Cy dyes, to insure that all solutions (including OA-caped UCNCs) have equal amount of UCNCs.
- Secondly, the amount of dissolved dyes was always monitored using absorption spectra.
- Thirdly, all samples were stored in a glove box, and the time between batch synthesis and completion of optical characterisation did not exceed 5 days. Moreover, dye-sensitised UCNCs obtained from one batch of OA-caped UCNCs were prepared and characterised within one day.

HCl treatment: The HCl treatment was used to remove oleate ligands from the surface of as-synthesized UCNCs. First, the toluene dispersed UCNCs were precipitated in acetone and centrifuged (2655 xg, 3 min) to collect white precipitate from the clear colorless supernatant. The supernatant was discarded, and the resulting white precipitate was dried in the air atmosphere. Then, 100 mg of dried UCNCs were dispersed in 10 mL water and HCl solution (0.1 M) was added dropwise, in such a way that the pH of the aqueous solution stabilizes at 4. The resulting mixture was stirred for 2 hours at room temperature. At the end of the HCl treatment process, OH groups substitute the oleate ligands on the surface of UCNCs, so the prepared ligand-free UCNCs are water-soluble. To remove the oleic acid and other byproducts of the HCl treatment process, 10 mL diethyl ether was added to the aqueous solution and the mixture stirred for one minute. The aqueous and organic solutions were extracted using an extraction funnel, then the aqueous solution was mixed again with 10 mL diethyl ether. The extraction process repeats three times, to be sure all organic residuals are removed from the surface of UCNCs. The obtained ligand-free UCNCs were precipitated by adding 15 mL acetone and centrifugation (2655 xg, 3 min). Finally, the supernatant was discarded and the purified UCNCs were dried in the air atmosphere.

Dye-sensitizing and purification processes in the air (measuring the dye:UCNCs ratio):

Different kinds of dye materials were separately dissolved in 10 mL MeOH for preparation of dye solution (different concentrations). The mixtures were stirred for 1 hour, then the absorption spectra of all dye solutions were measured in the 10 mm thickness cuvettes. Such data are providing the absorption-concentration ratio, as can also be approved by the dyes' molar absorptivity coefficients. The dye-sensitizing processes were performed by dispersing 4 mg of ligand-free UCNCs in different dyes' MeOH solutions (30 µg dye in 10 mL MeOH). The mixture was stirred for 1 hour at room temperature (air atmosphere). The dye-sensitized UCNCs were purified through five steps. Each purification step has consisted of centrifugation (2655

xg, 5 min), separation of precipitates and supernatant, and re-dispersing the precipitates in 10 mL MeOH. In each purification step, the absorption spectra of dye-sensitized UCNCs before centrifugation, and the absorption spectra of supernatant after centrifugation were measured using similar cuvettes. While both bound and unbound dyes participate in the absorption spectra of non-centrifuged samples, just unbound dyes are responsible for the absorption spectra of supernatant after the centrifugation process (It should also be noted that the absorption spectra of dye solutions before and after the centrifugation process were exactly same, indicating the dyes are not precipitating by centrifugation). So the difference in the absorption spectra of samples before and after centrifugation is a meter for measuring the concentration of bound dyes. On the other side, the concentration of ligand-free UCNCs in MeOH is 0.4 mg/mL in all samples. Therefore, considering the molar mass of different dyes and UCNCs (calculated based on the method reported in ^{6, 7}), the number of bound dyes per each UCNC was measured. Briefly, the concentration of ligand-free UCNCs (C_{UCNCs}) in all the solutions is calculated by $C_{UCNCs}=(m/M)/V$ equation, where m , M and V are the mass of UCNCs, molar mass of UCNCs, and volume of MeOH. On the other hand, the dyes concentrations (C_{Dye}) are calculated by measuring the dye adsorption, and transferring the values to the concentration by using the previously measured absorption-concentration ratios (and even with beer-lambert law equation, $C_{Dye}=A/\epsilon.l$, while A , ϵ and l are the absorption, molar absorptivity, and length of light path). Eventually, the dye:UCNCs ratios are calculated by dividing the dye concentration to UCNCs concentration ($dye:UCNCs = C_{Dye}/C_{UCNCs}$).

Optimized dye-sensitizing process in the air: Two MeOH solutions were prepared in the air atmosphere by dispersing the ligand-free UCNCs and dye materials in MeOH (MeOH). The concentration of Cy 740, Cy 754, Cy 784, Cy 792 dyes, and ligand-free UCNCs in MeOH solutions were 3.1, 2.6, 2.6, 2.5, and 4000 $\mu\text{g/mL}$, respectively. The dye-sensitizing process was performed by mixing 1 mL of ligand-free UCNCs in MeOH and 1 mL of dye solution in

the air atmosphere. The mixture was stirred for 1 hour at room temperature. After that, the solution was transferred to a cuvette for further optical measurements. The final concentration of all prepared samples was ~ 2 mg/mL.

Furthermore, to evaluate the effect of unbound dye molecules, the dye-sensitized UCNCs were purified through two steps. Each purification step was consisted of centrifugation (6797 xg, 5 min), discarding the supernatant, and re-dispersing the precipitates in 2 mL MeOH. After that, the solution was transferred to a cuvette for further optical measurements. The final concentration of all prepared samples was ~ 2 mg/mL.

Optimized dye-sensitizing process in Ar: Two solutions were prepared in a Schlenk line apparatus under Ar, by dispersing the ligand-free UCNCs and dye materials in CD₃OD. The concentration of Cy 740, Cy 754, Cy 784, Cy 792 dyes, and ligand-free UCNCs in CD₃OD solutions were 3.1, 2.6, 2.6, 2.5, and 4000 μ g/mL, respectively. The dye-sensitizing process was performed by mixing 1 mL of ligand-free UCNCs in CD₃OD and 1 mL of dye solution under Ar. The mixture was stirred for 1 hour at room temperature. After that, the solution was transferred to a cuvette, and sealed with a parafilm. The final concentration of all prepared samples was ~ 2 mg/mL.

8- Materials characterization

Transmission electron microscopy (TEM) and scanning transmission electron microscopy (STEM). The mean size, size distribution, and morphology of as-synthesized UCNCs were investigated by transmission electron microscopy (TEM) and high-angle annular dark-field (HAADF) scanning transmission electron microscopy (STEM) conducted with a FEI Osiris ChemiSTEM microscope at 200 keV electron energy. TEM samples were prepared at room temperature in air by drop-casting of 10 μ L diluted suspension of UCNCs in toluene onto an ultrathin carbon film (3 nm) on holey carbon support film mounted on 400 μ m mesh Cu grid (Ted Pella Inc.).

X-ray diffraction (XRD). The crystal structure of as-synthesized UCNCs was studied at room temperature using a D2Phaser diffractometer from Bruker (30 kV–10 mA), with Cu K α radiation ($\lambda = 1.5405 \text{ \AA}$) in Bragg-Brentano configuration.

Fourier transform infrared (FTIR). The presence of the organic components on the surface of UCNCs was studied using a Fourier transform infrared (FTIR) spectrometer (Vertex 70, Bruker).

Absorption spectra. UV/vis absorption spectra of UCNCs in toluene, dyes, and dye-sensitized UCNCs in methanol were measured using a Lambda 950 (PerkinElmer) spectrophotometer. The absorption spectra of all solutions were measured in 10 mm quartz cuvettes (Hellma Analytics) against the cuvette with the reference solvent.

Emission spectra. Photoluminescence emission spectra of all samples were recorded with a spectrometer (Avantes, AvaSpec-ULS2048 \times 64TEC). Emission was collected with a lens assembly (LA4725 and LA4148, Thorlabs) and guided into the spectrometer via an optical fiber (FP1000URT). A long-pass filter was placed between the sample and lens assembly (either FEL0650 or FEL0700, Thorlabs depending on the excitation wavelength). Tunable CW Ti-Sapphire laser (Solstis, M-Squared Lasers Ltd) pumped by 532 nm laser (Verdi-V18, Coherent) was used as an excitation source. The output power was 500mW in all cases, and the laser emission was focused on the sample with a lens providing a beam spot with area of 0.006 cm 2 and resulting intensity equal to 75 W/cm 2 . The laser beam size was measured with a beam profiler (Thorlabs, BP209-IR/M) by placing it in the same location as the sample in order to calculate excitation power density. The emission of dyes was recorded under 740 nm excitation. Cy 740, Cy 748, Cy 754, Cy 778, Cy 784, Cy 792-sensitized, and oleate-capped NCs were excited with 740 nm, 748 nm, 754 nm, 778 nm, 784 nm, 792 nm, and 980 nm laser emission, respectively.

9- Optimal composition of UCNCs

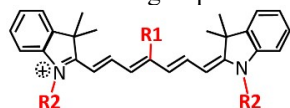
The composition of UCNCs can highly affect the dye triplet populations in such a way that the heavy lanthanide ions at the UCNCs surface significantly increase dye ISC and triplet states population. The optimum amount of heavy Gd^{3+} atoms on the composition of UCNCs was measured around 30%, while the higher amounts can cause the interaction of Gd^{3+} - Yb^{3+} - Er^{3+} optical characteristics and so faster energy migration to the surface traps⁸. In this regard, (β - $NaY_{0.5}Gd_{0.3}F_4:Yb_{0.18},Er_{0.02}$ UCNCs were synthesized for further evaluating the triplet population in our synthesized cyanine dyes, and subsequently UC luminescence enhancement of dye-sensitized UCNCs. The TEM images and also particle size distribution histogram of **Fig. S17** indicate that the synthesized UCNCs are highly monodispersed, and have an elliptical morphology with an average dimension of 18.2×23.8 nm. The XRD pattern of **Fig. S18** also confirms the synthesis of hexagonal β -phase. According to **Fig. S19**, sensitizing the (β - $NaY_{0.5}Gd_{0.3}F_4:Yb_{0.18},Er_{0.02}$ UCNCs with cyanide dyes results in a significant UC luminescence enhancement, in such a manner that the red emission peaks of the dye-sensitized UCNCs appeared at 654 nm (the red emission of UCNCs is stronger than the dyes anti-Stokes shoulder around 650 nm). In this case, the emission intensities of Cy 740- and Cy 754-sensitized UCNCs are 10- and 4-times higher than those of sensitized $NaGd_{0.8}F_4:Yb_{0.18},Er_{0.02}$ UCNCs, respectively (excitation wavelengths of 740 and 754 nm). As indicated in **Fig. S20**, the dye-sensitized $NaY_{0.5}Gd_{0.3}F_4:Yb_{0.18},Er_{0.02}$ UCNCs have much higher absorption intensities than the previously sensitized $NaGd_{0.8}F_4:Yb_{0.18},Er_{0.02}$, since the bigger $NaY_{0.5}Gd_{0.3}F_4:Yb_{0.18},Er_{0.02}$ UCNCs can be coordinated with a higher number of dye molecules. Respected, the higher UC luminescence enhancement of all dye-sensitized $NaY_{0.5}Gd_{0.3}F_4:Yb_{0.18},Er_{0.02}$ UCNCs can also be explained by both the effects of a large size of UCNCs, as well as higher triplet populations by the UCNCs of optimum composition.

10- Supplementary table

Table S1. Chemical structure and photophysical properties of the synthetic cyanine dyes.

	Chemical formula	R1*	R2*	$\lambda_{\text{Absorption}}$ (nm)	$\lambda_{\text{Emission}}$ (nm)	Molar mass (g/mol)
Cy 740	C ₃₃ H ₃₇ N ₂ O ₆ S ₂ INa	-I	-SO ₃	740	774	771.10
Cy 748	C ₃₀ H ₃₃ N ₂ O ₂ I	-COOH	-H, I-	748	787	580.51
Cy 754	C ₃₄ H ₃₈ N ₂ O ₈ S ₂ Na	-COOH	-SO ₃ -	754	794	689.19
Cy 778	C ₃₁ H ₃₅ N ₂ O ₂ I	-COOCH ₃	-H, I-	778	866	594.50
Cy 784	C ₄₃ H ₄₇ N ₂ O ₆ S ₂ Na	-H	-SO ₃ -	784	830	774.96
Cy 792	C ₄₂ H ₄₃ N ₂ O ₈ S ₂ Na	-COOH	-SO ₃ -	792	837	790.92

* Functional groups of the cyanine dyes with typical structure of below:



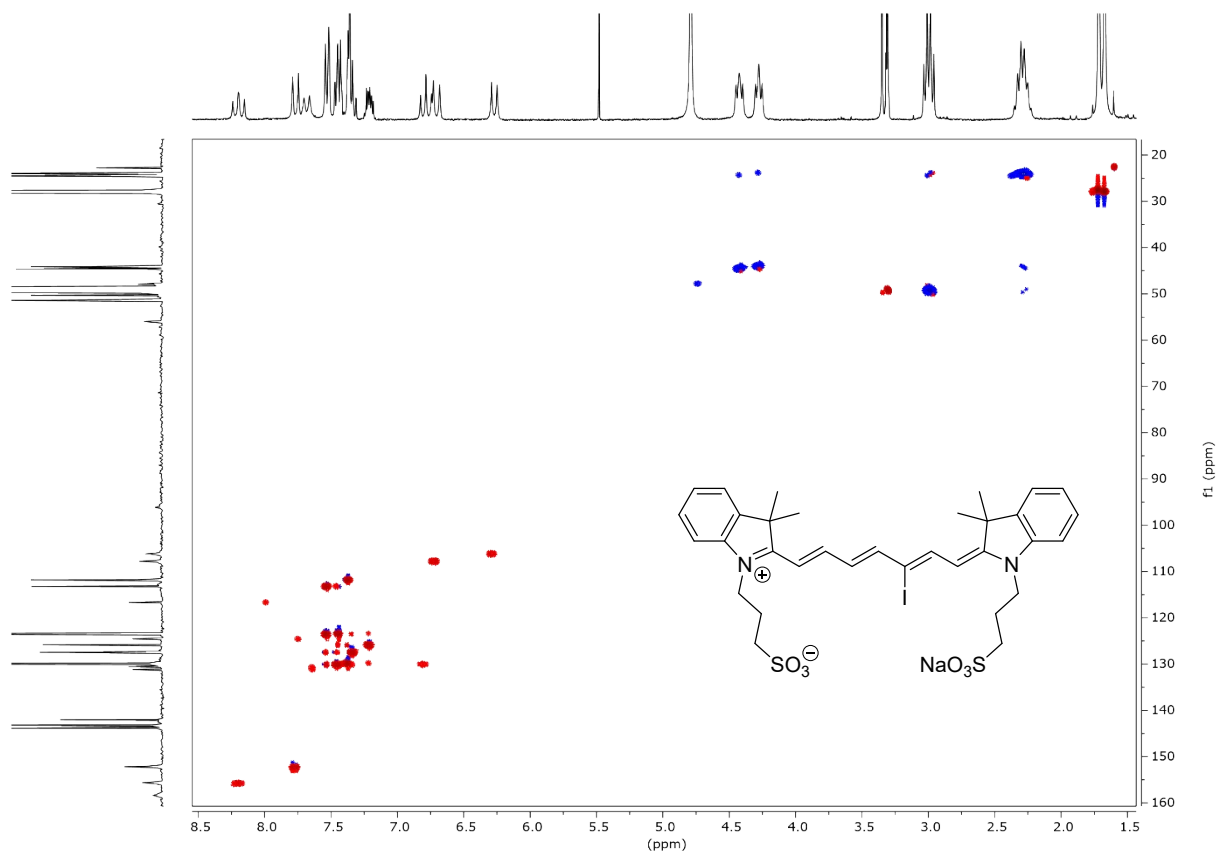


Fig. S3. ^1H - ^{13}C gHSQC (500 MHz, d_4 - CD_3OD): Cy 740.

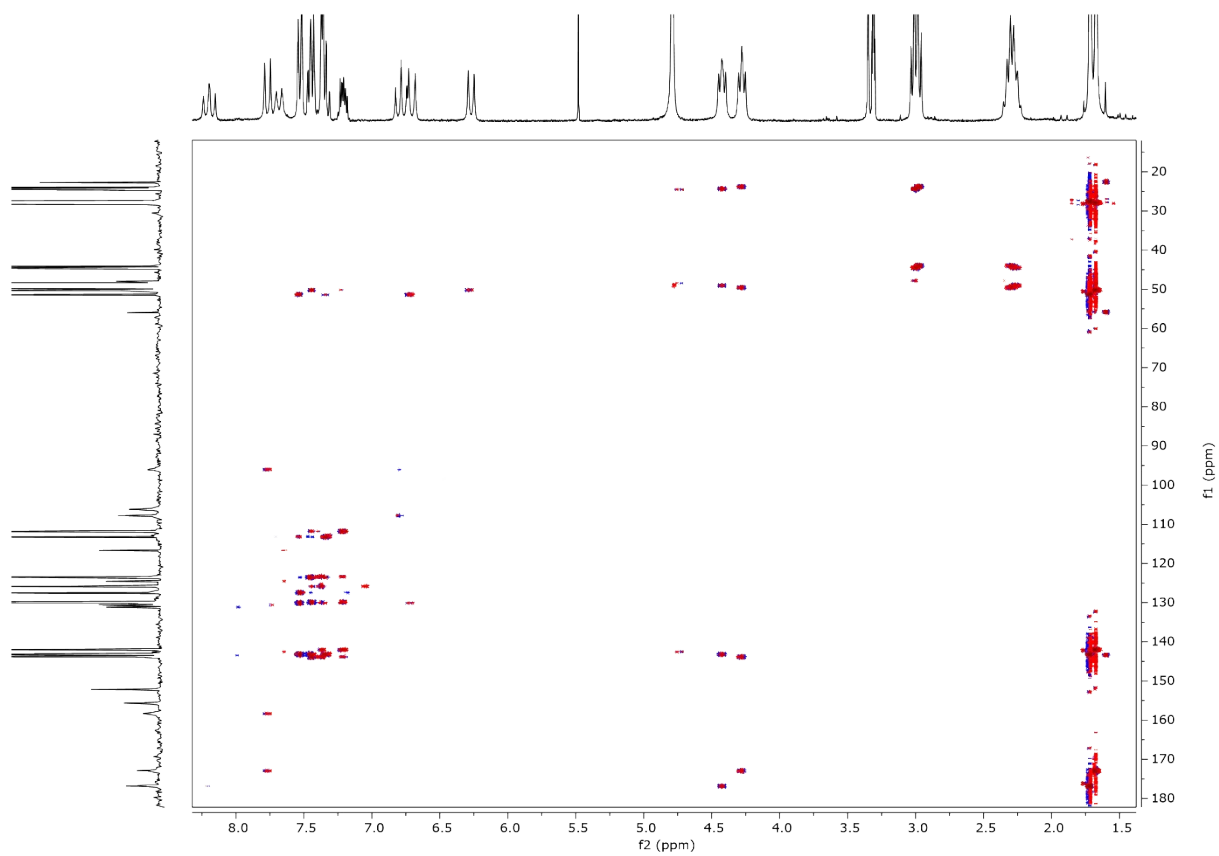


Fig. S4. ^1H - ^{13}C gHMBC (500 MHz, d_4 - CD_3OD): Cy 740.

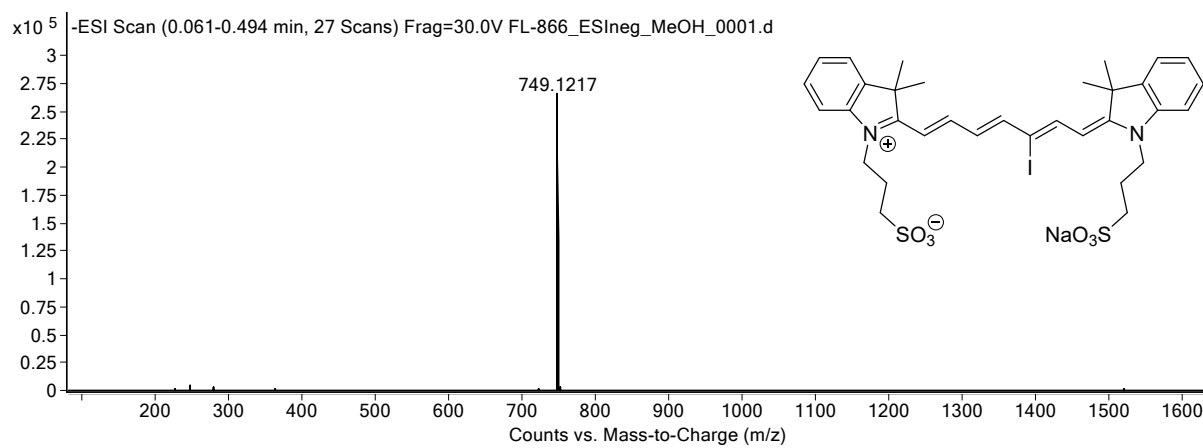


Fig. S5. HRMS (ESI⁻) m/z for **Cy 740**: $[M - Na^+]$ calcd for $C_{33}H_{38}IN_2O_6S_2^-$ 749.1221, found

749.1217

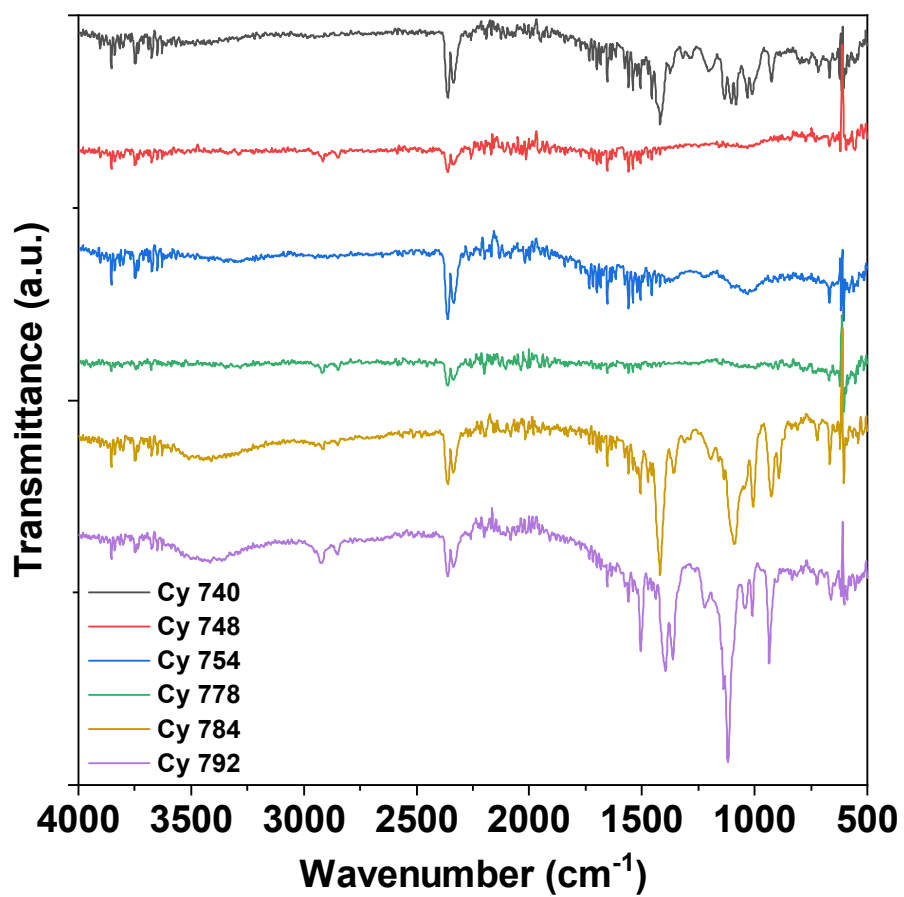


Fig. S6. FTIR spectra of the cyanine dyes.

After two purification steps, the supernatant shows no presence of dissolved free dyes. All dyes are firmly bound to the surface of the UCNCs.

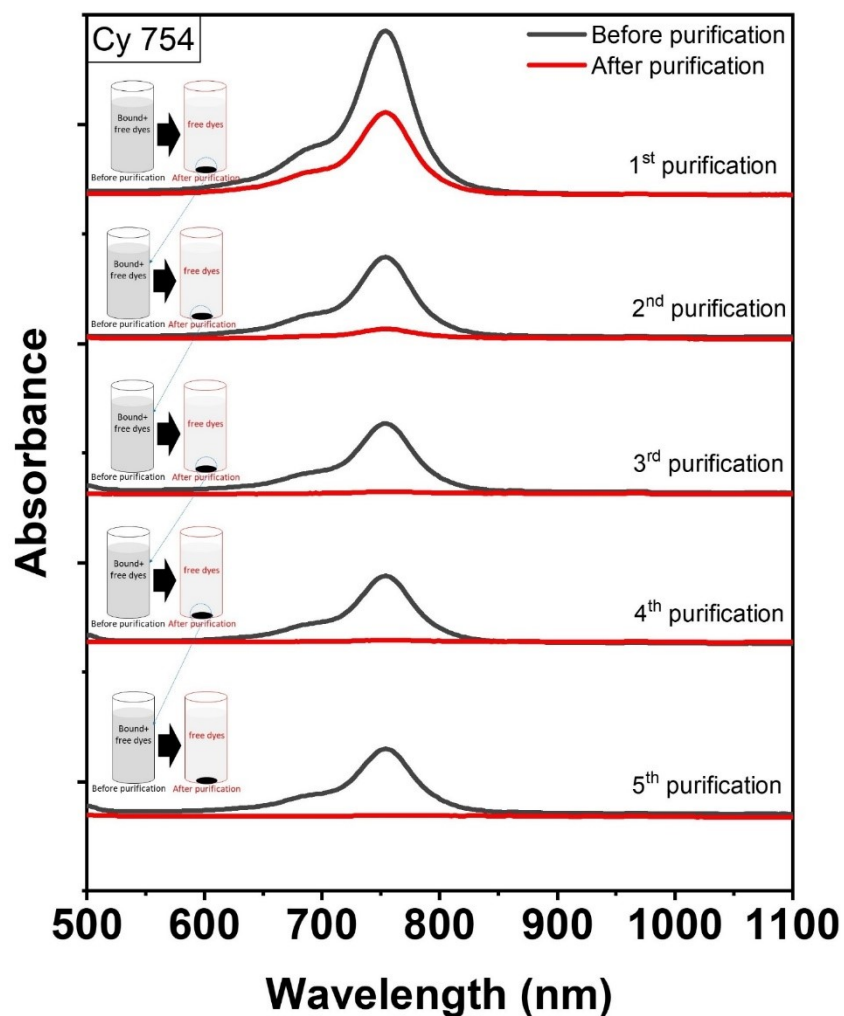


Fig. S7. Absorption spectra of MeOH solutions of Cy 754-capped $\text{NaGdF}_4:\text{Yb}^{3+},\text{Er}^{3+}$ UCNCs during five steps of purification processes. The black and red curves respectively represent the absorption spectra of the solution before purification and absorption spectra of supernatant after centrifugation processes.

After two purification steps, the supernatant shows no presence of dissolved free dyes. All dyes are firmly bound to the surface of the UCNCs.

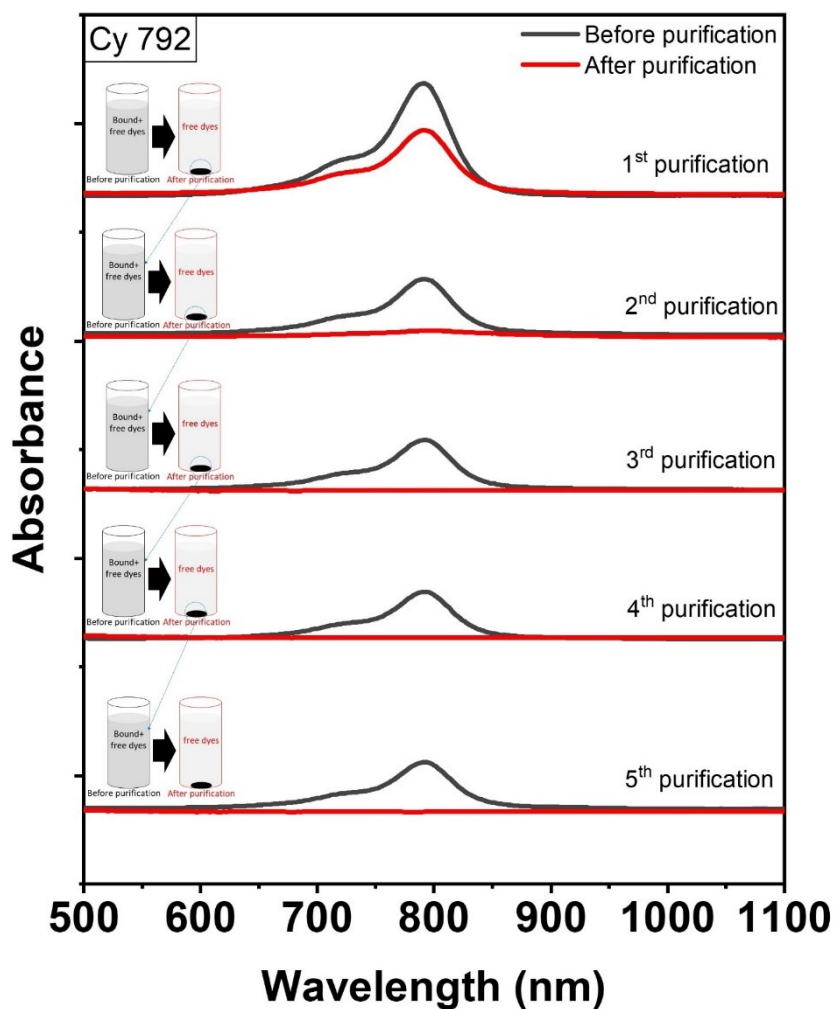


Fig. S8. Absorption spectra of MeOH solutions of Cy 792-capped $\text{NaGdF}_4:\text{Yb}^{3+},\text{Er}^{3+}$ UCNCs during five steps of purification processes. The black and red curves respectively represent the absorption spectra of the solution before purification and absorption spectra of supernatant after centrifugation processes.

After two purification steps, both the supernatant and the solution contain no dissolved free dyes. The dye is completely removed, indicating no strong interaction between dyes and UCNCs.

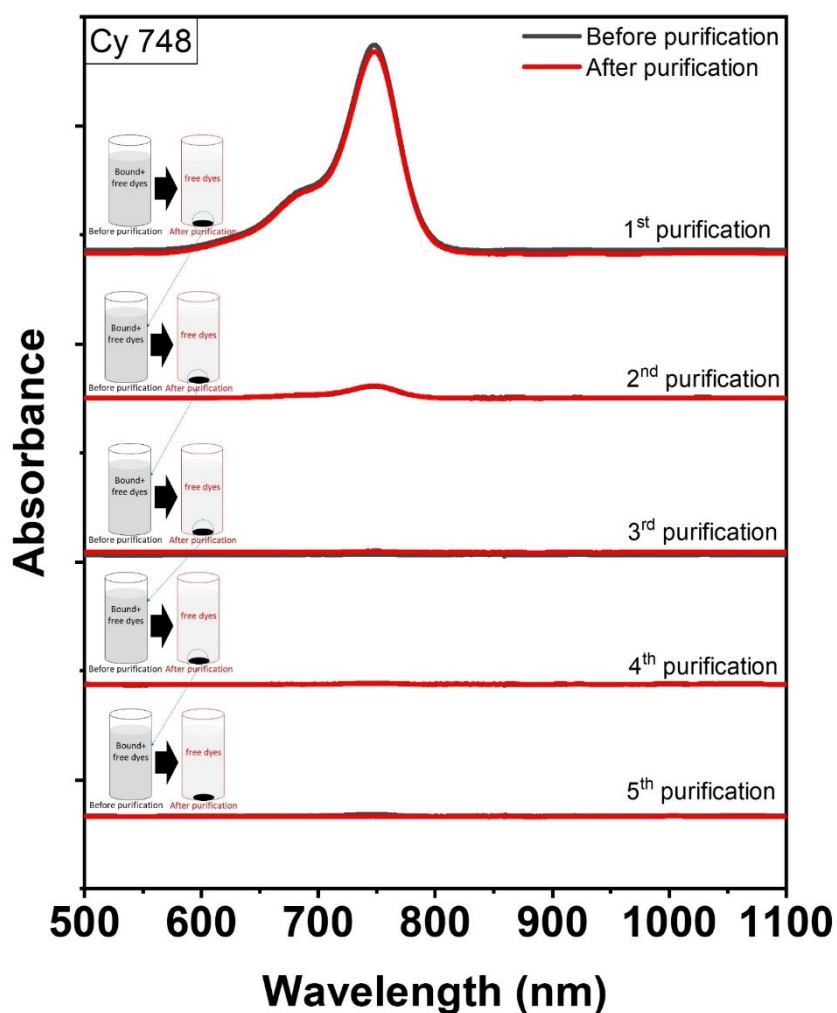


Fig. S9. Absorption spectra of MeOH solutions of Cy 748-capped NaGdF₄:Yb³⁺,Er³⁺ UCNCs during five steps of purification processes. The black and red curves respectively represent the absorption spectra of the solution before purification and absorption spectra of supernatant after centrifugation processes.

After two purification steps, both the supernatant and the solution contain no dissolved free dyes. The dye is completely removed, indicating no strong interaction between dyes and UCNCs.

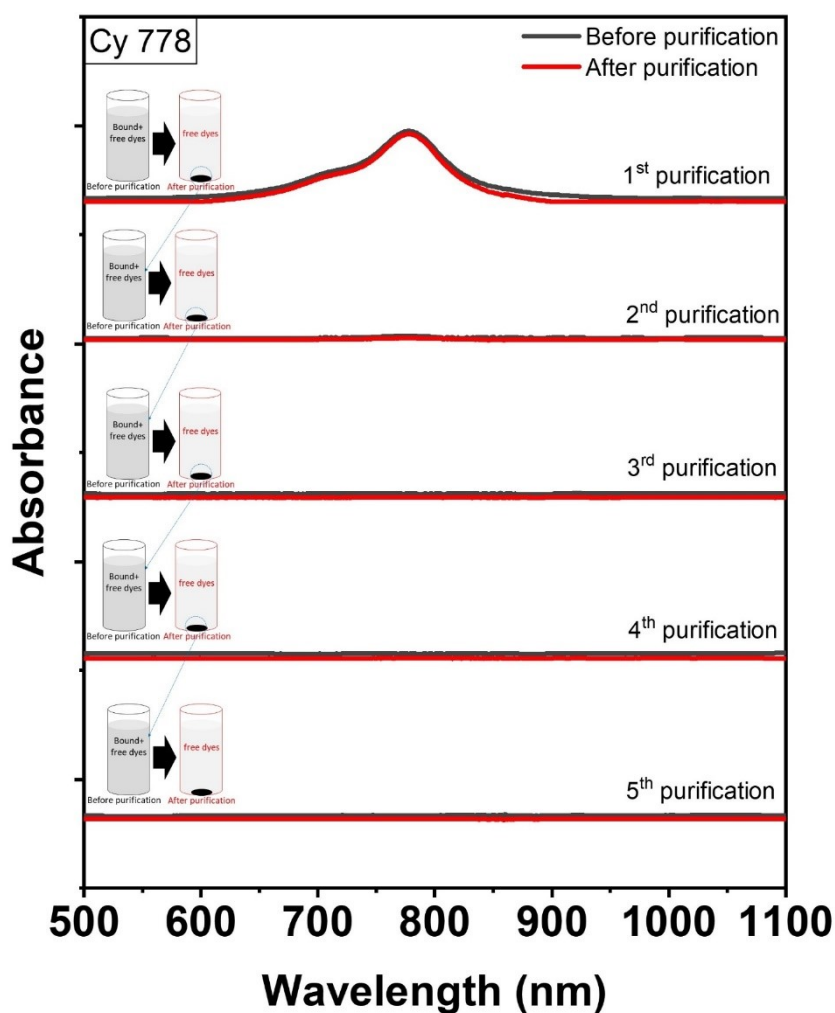


Fig. S10. Absorption spectra of MeOH solutions of Cy 778-capped NaGdF₄:Yb³⁺,Er³⁺ UCNCs during five steps of purification processes. The black and red curves respectively represent the absorption spectra of the solution before purification and absorption spectra of supernatant after centrifugation processes.

The dye is detected in the supernatant during the five purification steps. This indicates an equilibrium between adsorbed and free dye in solution.

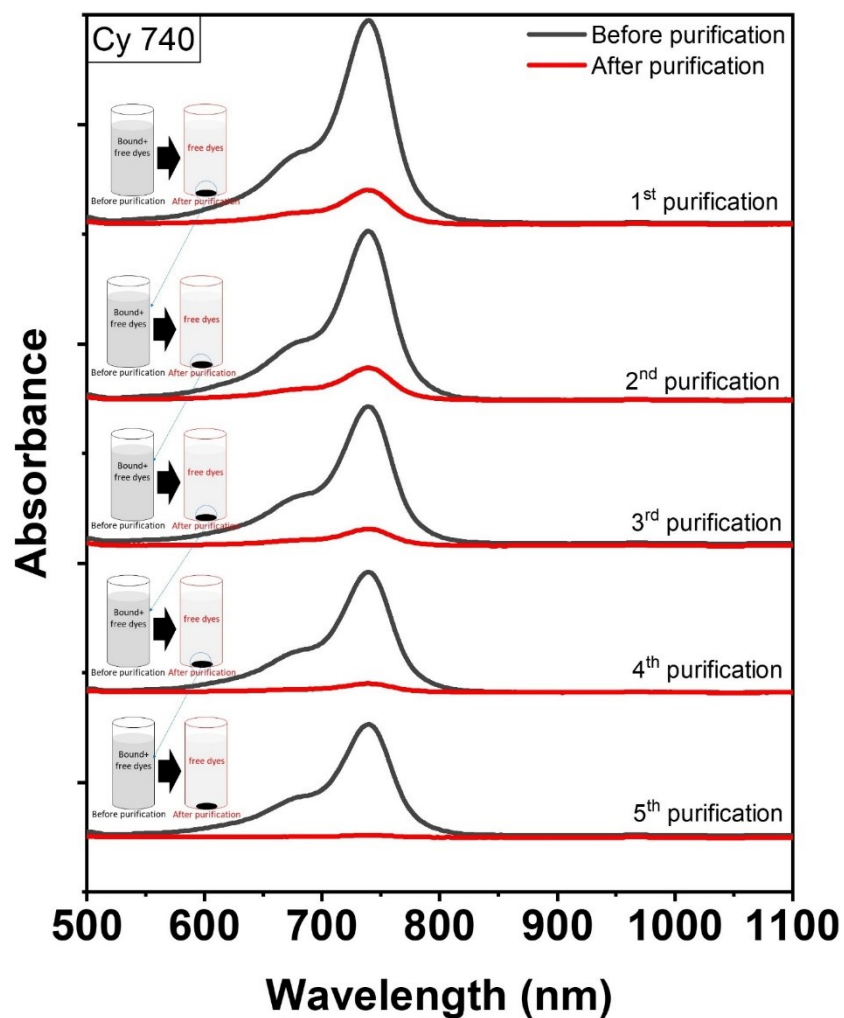


Fig. S11. Absorption spectra of MeOH solutions of Cy 740-capped $\text{NaGdF}_4:\text{Yb}^{3+},\text{Er}^{3+}$ UCNCs during five steps of purification processes. The black and red curves respectively represent the absorption spectra of the solution before purification and absorption spectra of supernatant after centrifugation processes.

The dye is detected in the supernatant during the five purification steps. This indicates an equilibrium between adsorbed and free dye in solution.

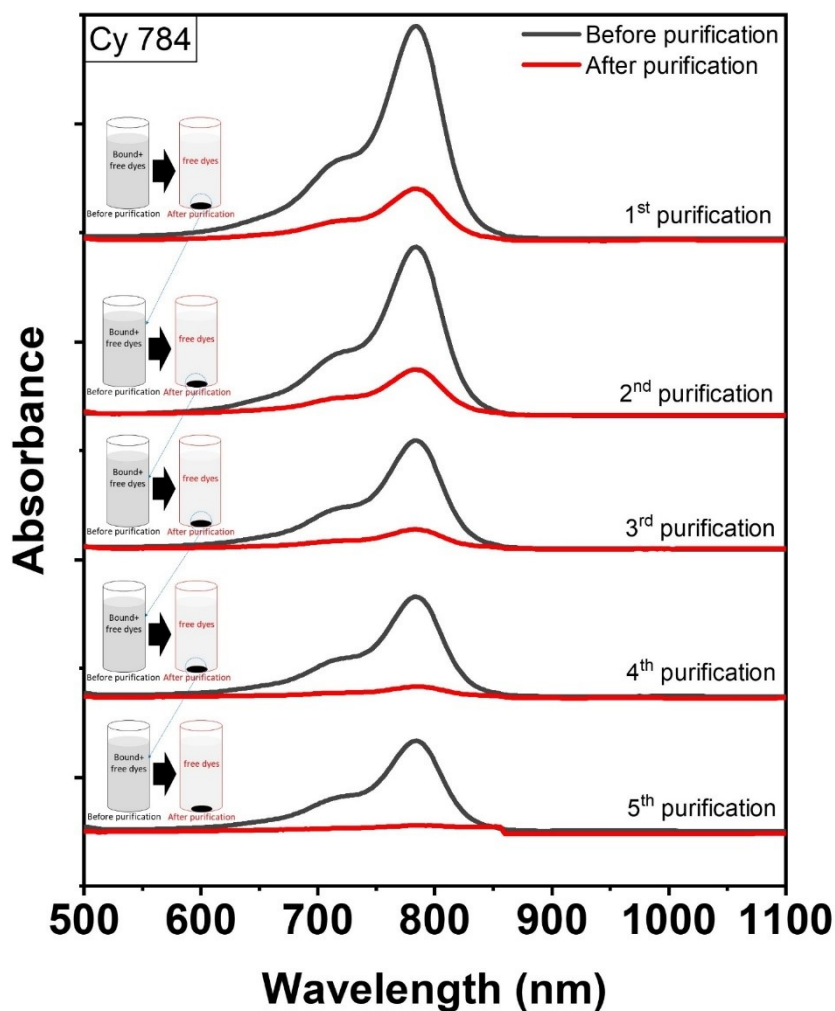


Fig. S12. Absorption spectra of MeOH solutions of Cy 784-capped $\text{NaGdF}_4:\text{Yb}^{3+},\text{Er}^{3+}$ UCNCs during five steps of purification processes. The black and red curves respectively represent the absorption spectra of the solution before purification and absorption spectra of supernatant after centrifugation processes.

FTIR spectra show the presence of hydroxyl groups on the surface of all synthesized UCNCs.

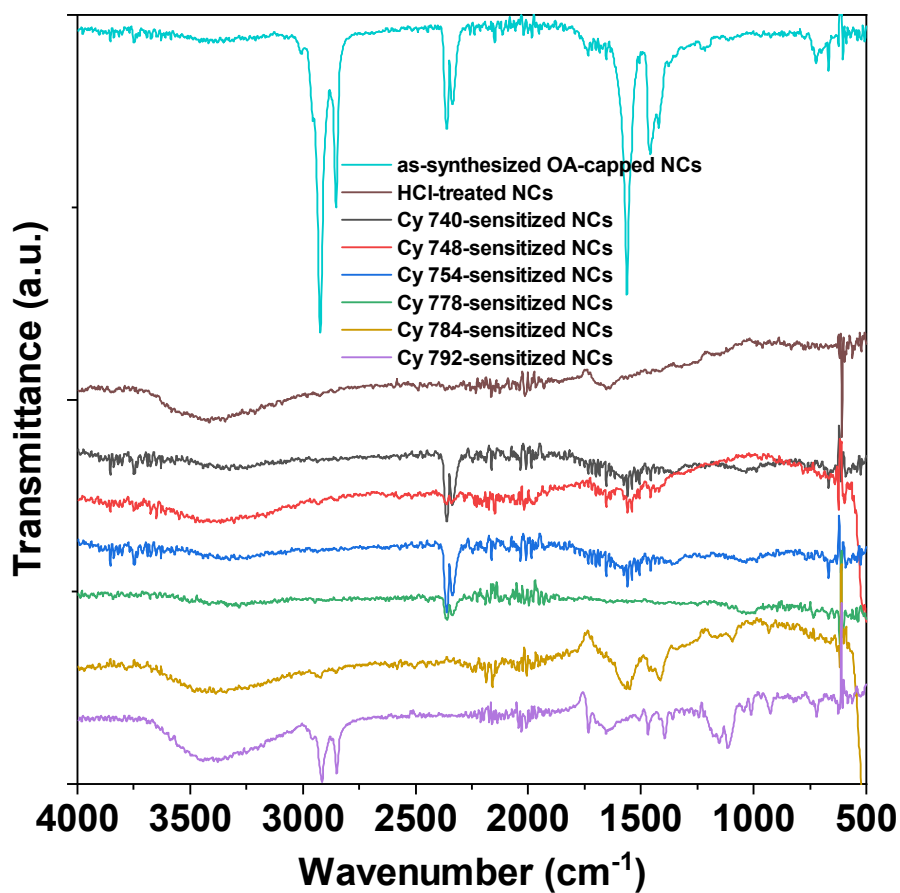


Fig. S13. FTIR spectra of the as-synthesized oleate-capped NaGdF₄:Yb³⁺,Er³⁺ UCNCs, HCl-treated, and different dye-sensitized UCNCs after 5 purification steps. As a result of HCl treatment, OH⁻ groups completely replaced the oleate ligands on the surface of UCNCs. The vibrational OH bands (3200-3600 cm⁻¹) are still strongly obvious in the spectra of dye-sensitized UCNCs.

In order to find the optimum ratio between dye and UC NCs, the UC intensity was measured at a fixed concentration of UCNCs and a variable concentration of dye. The UC intensity of different dye-sensitized UCNCs increases with increasing the dye concentrations until a certain maximum value is achieved. After that, increasing the dye concentrations resulted in a reduced BUC value, because the excess free dyes do not transfer energy to Yb^{3+} ions but instead reabsorb both the red and green UC radiation.

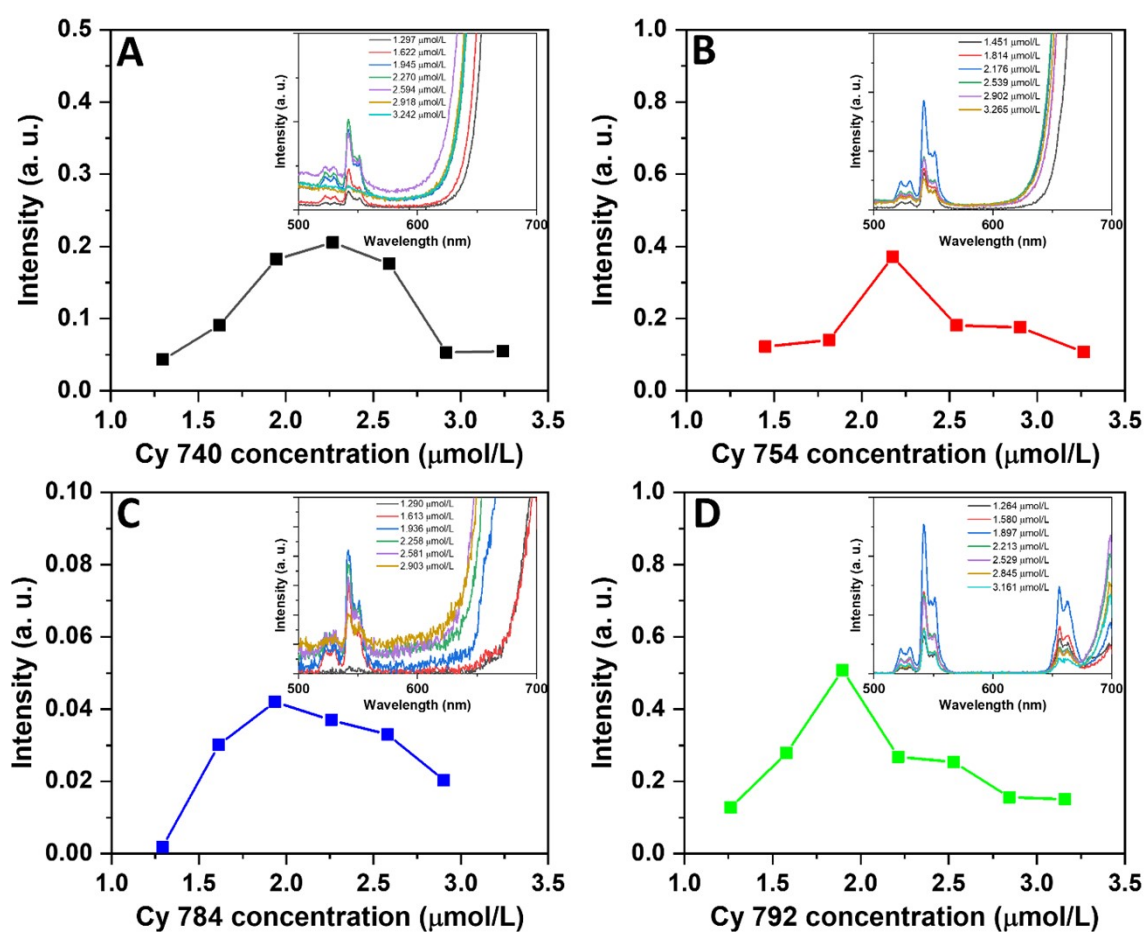


Fig. S14. UC intensity variations for Cy 740-capped (A), Cy 754-capped (B), Cy 784-capped (C), and Cy 792-capped (D) UCNCs at different dye concentrations ($\lambda_{\text{ex.}} = 740 \text{ nm}, 754 \text{ nm}, 784 \text{ nm}, \text{ and } 792 \text{ nm}$, respectively). The conjugation process was performed by mixing 1 mL of ligand-free UCNCs in MeOH (4 mg/mL) and 1 mL of dye MeOH solution (different concentrations of 2-5 $\mu\text{g/mL}$) in the air atmosphere, and without further purification processes.

The absorbance values corresponding to the laser wavelengths 740, 754, 784 and 792 nm were used to calculate the brightness (B_{UC}) and its variation.

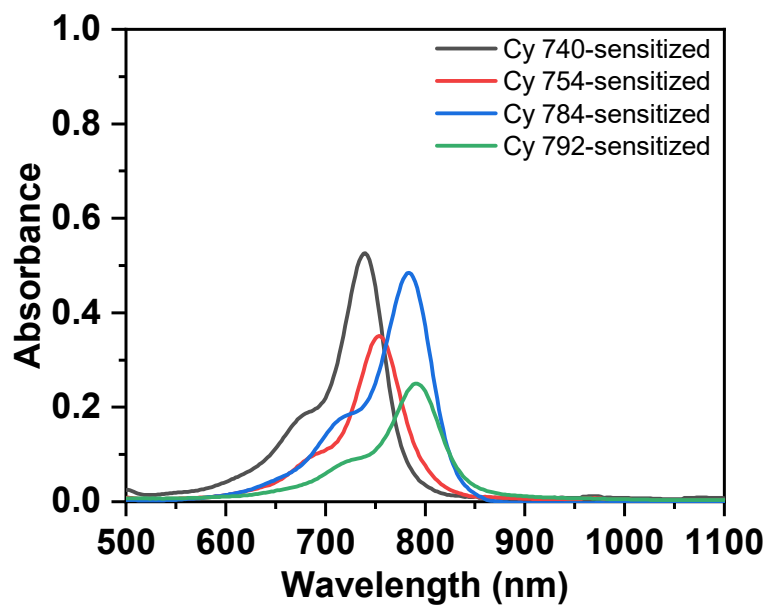


Fig. S15. Absorption spectra of different dye-capped $\text{NaGdF}_4:\text{Yb}^{3+},\text{Er}^{3+}$ UCNCs in CD_3OD . The conjugation with dyes was done under Ar, using the optimum dye:UCNCs ratio, and without further purification processes. The UC spectra were presented in Fig. S15.

The absorbance values corresponding to the laser wavelengths 740, 754, 784 and 792 nm were used to calculate the brightness (B_{UC}) and its variation.

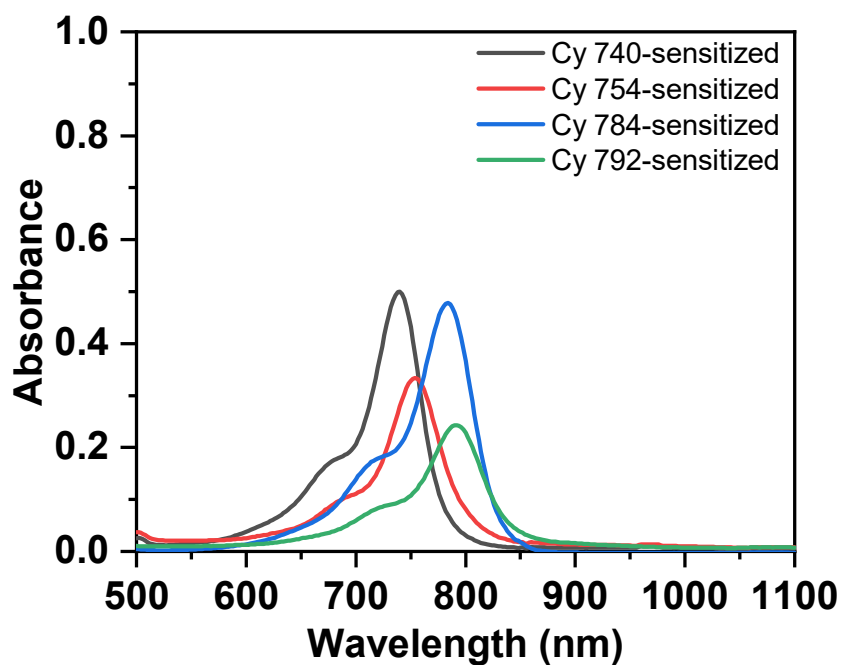


Fig. S16. Absorption spectra of different dye-capped NaGdF₄:Yb³⁺,Er³⁺ UCNCs in MeOH. The conjugation with dyes was done in the air, using the optimum dye:UCNCs ratio, and without further purification processes. The UC spectra were presented in Fig. S17.

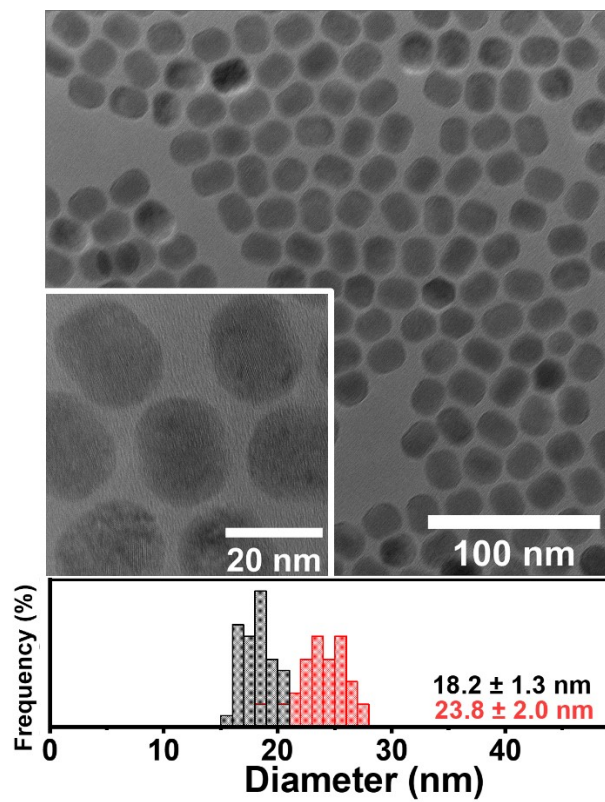


Fig. S17. Transmission electron microscopy micrographs and size distribution histogram for short (black) and long-axis (red) dimensions of NaY(Gd)F₄:Yb³⁺,Er³⁺ UCNCs.

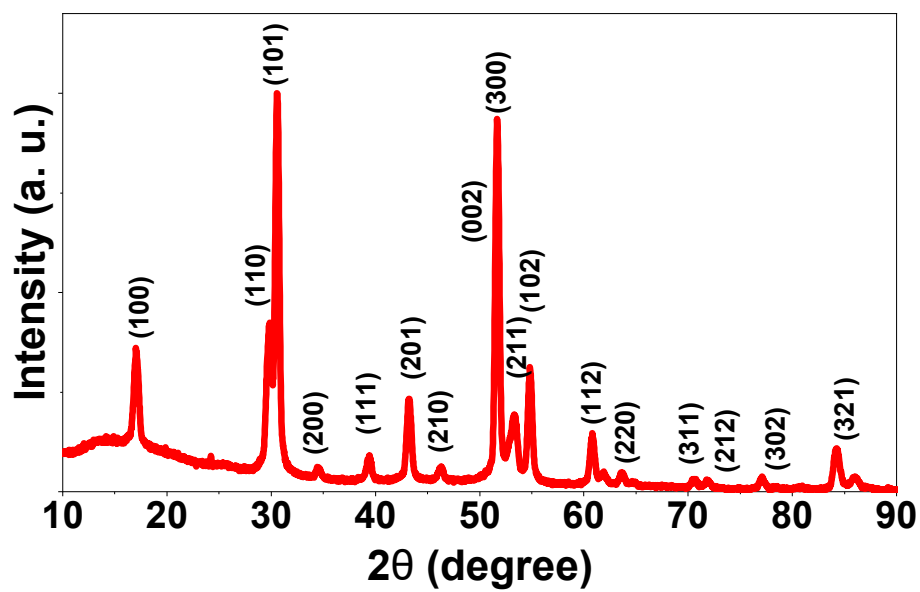


Fig. S18. X-ray diffraction pattern of $\text{NaY}(\text{Gd})\text{F}_4:\text{Yb}^{3+},\text{Er}^{3+}$ UCNCs.

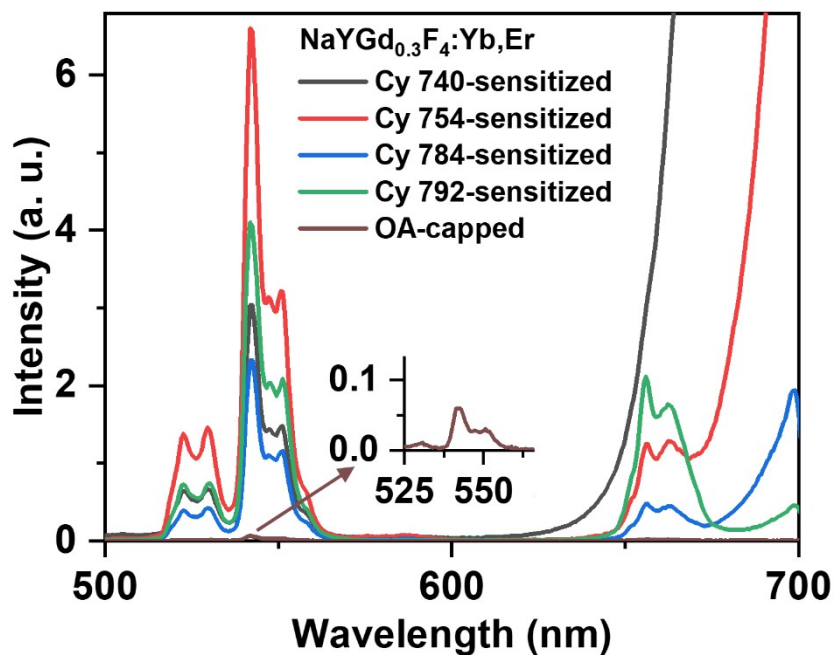


Fig. S19. UC luminescence spectra of different dye-capped NaY(Gd)F₄:Yb³⁺,Er³⁺ UCNCs in CD₃OD. The conjugation with dyes was done in the air, using the optimum dye:UCNCs ratio, using the optimum dye:UCNCs ratio, and without further purification processes. Cy 740-, Cy 754-, Cy 784-, Cy 792-, and OA-capped UCNCs were excited with 740, 754, 784, 792, and 980 nm lasers, respectively (excitation power of 75 W/cm²).

The absorbance values corresponding to the laser wavelengths 740, 754, 784 and 792 nm were used to calculate the brightness (B_{UC}) and its variation.

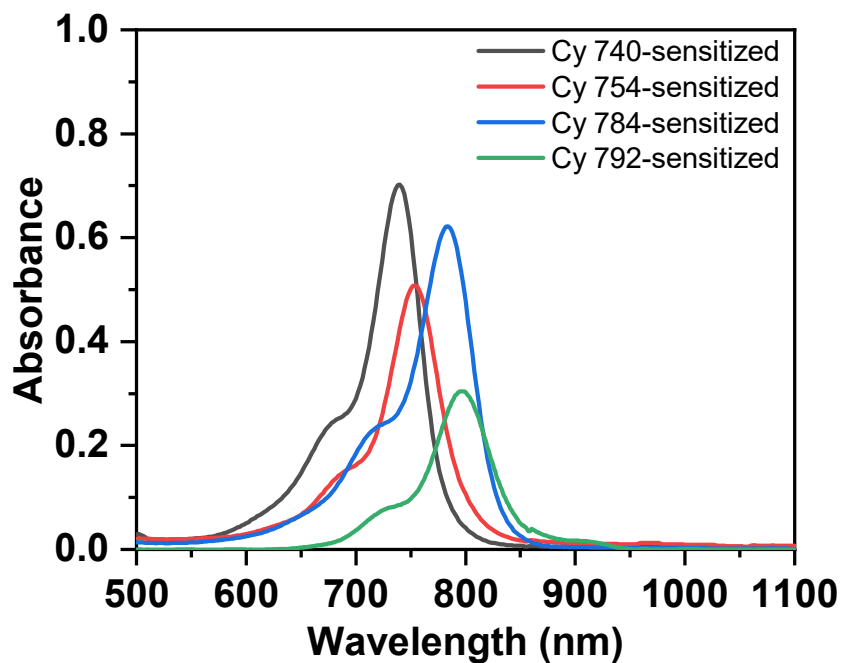


Fig. S20. Absorption spectra of different dye-sensitized NaY(Gd)F₄:Yb³⁺,Er³⁺ UCNCs in CD₃OD. The dye-sensitization was done under Ar and without further purification processes.

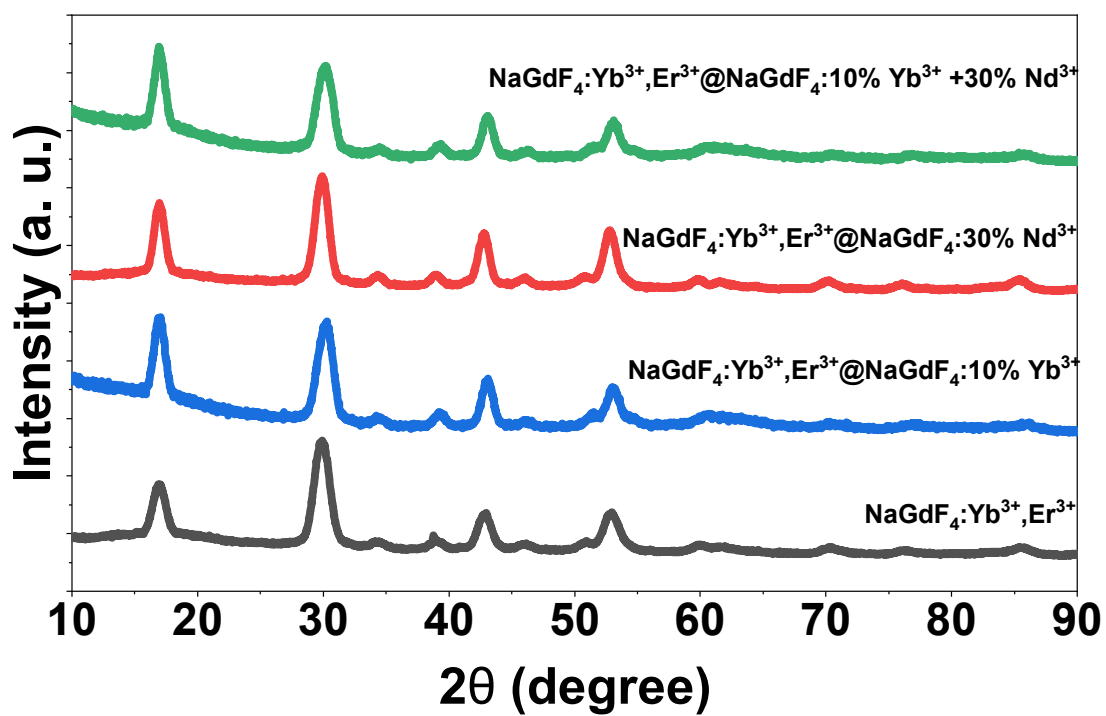


Fig. S21. XRD patterns of $\text{NaGdF}_4:\text{Yb}^{3+},\text{Er}^{3+}$ core and $\text{NaGdF}_4:\text{Yb}^{3+},\text{Er}^{3+}@ \text{NaGdF}_4:\text{Ln}^{3+}$ core@shell UCNCs.

The absorbance values corresponding to the laser wavelengths 740, 754, 784 and 792 nm were used to calculate the brightness (B_{UC}) and its variation.

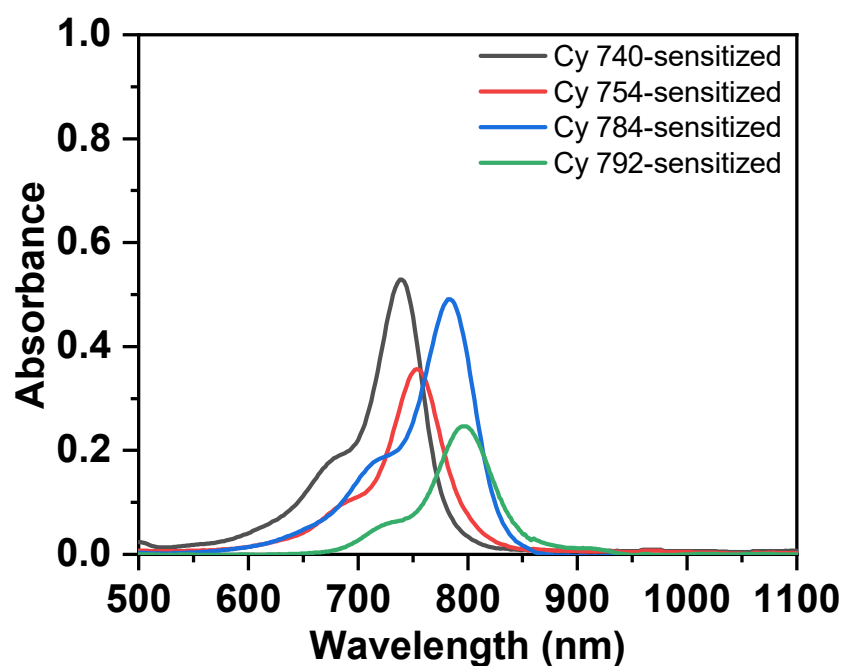


Fig. S22. Absorption spectra of dye-capped NaGdF₄:Yb³⁺,Er³⁺@NaGdF₄:10%Yb³⁺ core@shell UCNCs.

The absorbance values corresponding to the laser wavelengths 740, 754, 784 and 792 nm were used to calculate the brightness (B_{UC}) and its variation.

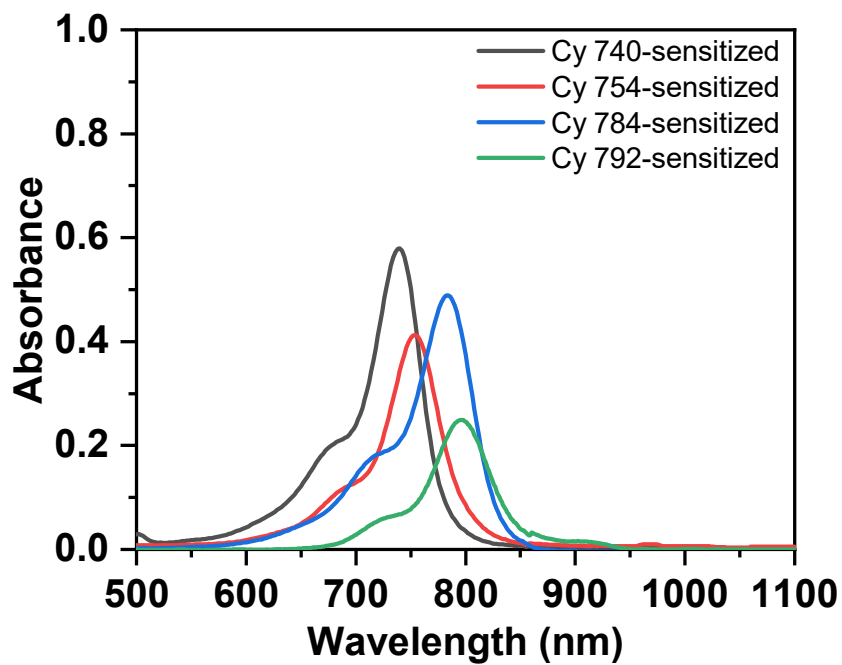


Fig. S23. Absorption spectra of dye-capped NaGdF₄:Yb³⁺,Er³⁺@NaGdF₄:30%Nd³⁺ core@shell UCNCs.

The absorbance values corresponding to the laser wavelengths 740, 754, 784 and 792 nm were used to calculate the brightness (B_{UC}) and its variation.

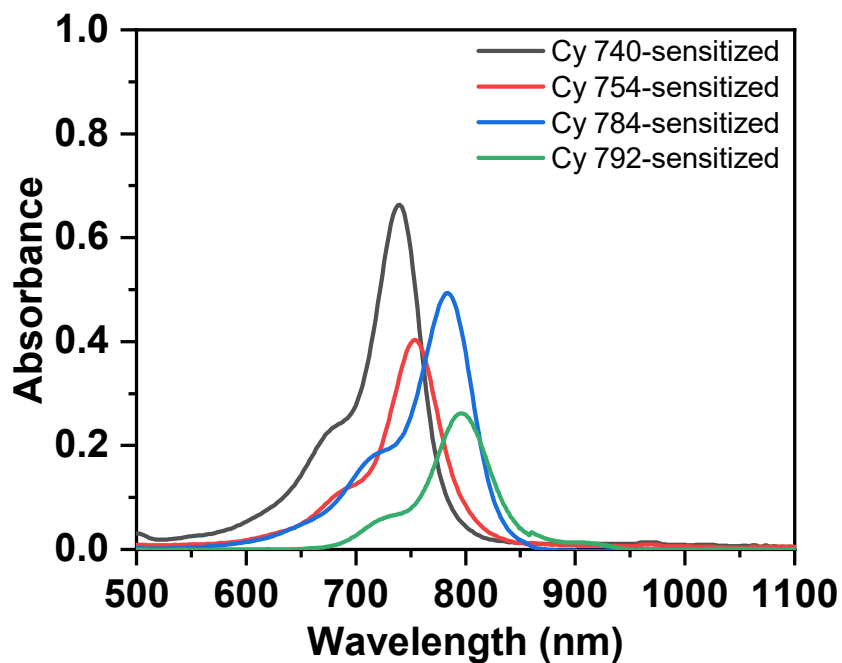


Fig. S24. Absorption spectra of dye-capped $\text{NaGdF}_4:\text{Yb}^{3+},\text{Er}^{3+}@\text{NaGdF}_4:10\%\text{Yb}^{3+}+30\%\text{Nd}^{3+}$ core@shell UCNCs.

Doping the Nd^{3+} ions into the shell layer causes a strong absorption of core@shell UCNCs in the range 725 – 900 nm.

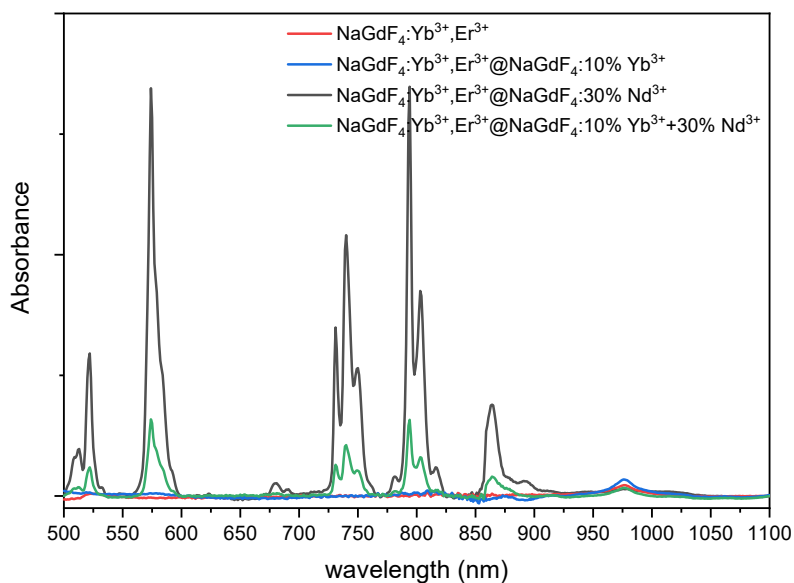


Fig. S25. Absorption spectra of $\text{NaGdF}_4:\text{Yb}^{3+},\text{Er}^{3+}$ core and $\text{NaGdF}_4:\text{Yb}^{3+},\text{Er}^{3+}@ \text{NaGdF}_4:\text{Ln}^{3+}$ core@shell UCNCs. The absorption peaks at 740, 800, and 860 nm correspond to the ground state absorption to the $^4\text{S}_{3/2}/^4\text{S}_{7/2}$, the $^4\text{F}_{5/2}/^2\text{H}_{9/2}$, and the $^4\text{F}_{3/2}$ states of Nd^{3+} ions, respectively, while the absorption peak at ~ 980 nm corresponds to the $^2\text{F}_{7/2} \rightarrow ^2\text{F}_{5/2}$ transition of Yb^{3+} ions.

References

1. L. Šťacková, P. Šťacko and P. Klán, *Journal of the American Chemical Society*, 2019, **141**, 7155.
2. <https://gaussian.com/citation/>.
3. F. Wang, R. Deng and X. Liu, *Nature protocols*, 2014, **9**, 1634.
4. D. Hudry, D. Busko, R. Popescu, D. Gerthsen, A. M. Abeykoon, C. Kübel, T. Bergfeldt and B. S. Richards, *Chemistry of Materials*, 2017, **29**, 9238.
5. L. Šťacková, P. Šťacko and P. Klán, *Journal of the American Chemical Society*, 2019, **141**, 7155.
6. W. Wei, G. Chen, A. Baev, G. S. He, W. Shao, J. Damasco and P. N. Prasad, *Journal of the American Chemical Society*, 2016, **138**, 15130.
7. G. Chen, J. Damasco, H. Qiu, W. Shao, T. Y. Ohulchanskyy, R. R. Valiev, X. Wu, G. Han, Y. Wang and C. Yang, *Nano letters*, 2015, **15**, 7400.
8. D. J. Garfield, N. J. Borys, S. M. Hamed, N. A. Torquato, C. A. Tajon, B. Tian, B. Shevitski, E. S. Barnard, Y. D. Suh and S. Aloni, *Nature Photonics*, 2018, **12**, 402.